Thermal spin transition in [Fe(NH2-trz)3]Br2 investigated by spectroscopic ellipsometry

E. D. Loutete-Dangui, François Varret, Epiphane Codjovi, Pierre-Richard Dahoo, Hiroko Tokoro, Shin-Ichi Ohkoshi, C. Eypert, Jean-François Létard, J. M. Coanga, K. Boukheddaden

Thermal spin transition in $[Fe(NH_2\text{-}trz)_3]Br_2$ investigated by spectroscopic ellipsometry

E. D. Loutete-Dangui,[1] F. Varret,[1] E. Codjovi,[1] P. R. Dahoo,[2] H. Tokoro,[3] S. Ohkoshi,[3] C. Eypert,[4] J. F. Létard,[5] J. M. Coanga,[2] and K. Boukheddaden[1,*]

[1]*Groupe d'Etudes de la Matière Condensée, CNRS—Université de Versailles St. Quentin en Yvelines, 45 Avenue des États Unis, F78035 Versailles Cedex, France*

[2]*Département de Physique, Université de Versailles St. Quentin en Yvelines, UVSQ, 45 Avenue des États Unis, 78 035 Versailles Cedex, France*

[3]*Department of Chemistry, School of Science, University of Tokyo, 7-3-1, Hongo, Bunkyo-ku, Tokyo, 113-0033, Japan*

[4]*Division Couches Minces, HORIBA Jobin Yvon SAS, Z. A. de la vigne aux Loups, 5 avenue Arago, 91380 Chilly-Mazarin, France*

[5]*Institut de Chimie de la Matière Condensée de Bordeaux (ICMCB), CNRS UPR 9048, Groupe des Sciences Moléculaires, Université Bordeaux I, 87 Avenue du Docteur Schweitzer, 33608 Pessac Cedex, France*

(Received 9 January 2007; revised manuscript received 4 April 2007; published 21 May 2007)

We investigated the thermal hysteresis of a pelleted sample of the spin-crossover compound $[Fe(NH_2\text{-}trz)_3]Br_2$ by means of spectroscopic ellipsometry, in the temperature range 264–358 K. The ellipsometric parameters (ψ,Δ) have been recorded in the optical range 240–1000 nm. The corresponding absorption and dispersion spectra show temperature-invariant isobestic points located at 240 and 291 nm, respectively. We found that the high-spin-fraction data, derived from the integrated absorption curves, are in excellent agreement with the magnetic data recorded on the same sample. We also investigated the consistency of the optical data by application of the Kramers-Kronig relations, which are well obeyed above ~450 nm. All these results demonstrate that the spectroscopic ellipsometry is well adapted to characterize the spin-crossover transition. We also expect that this nondestructive technique will be highly relevant to investigate the physical properties of thin films of switchable molecular solids, involving a change in the electronic properties upon a thermally or photoinduced phase transition.

DOI: 10.1103/PhysRevB.75.184425 PACS number(s): 47.51.+a

I. INTRODUCTION

In recent years, there has been growing interest in the field of the spin-crossover (SC) materials, which under various constraints, such as temperature variations,[1] pressure,[2–4] light irradiation,[5–9] or magnetic field,[10] show a transition between low-spin (LS) and high-spin (HS) states.[11,12] For example, Fe(II) SC materials[13] are diamagnetic ($S=0$, LS) and paramagnetic ($S=2$, HS) in the low- and high-temperature phases, respectively. Upon the spin crossover, these Fe(II) complexes undergo drastic variation of the metal-ligand bond lengths (≃0.2 Å, i.e., ≃10%) and ligand-metal-ligand bond angles (0.5°–8°),[6,14] accompanied by important changes in the electronic (spin-state) structure and orbital occupancy. Appreciable changes in optical properties result, for example the color[5,15,16] changes from purple to light yellow when the title compound undergoes the LS→HS transition, that is, on heating. Consequently, magnetic and optical measurements[17–20] are the major experimental techniques used for quantitative investigations of the spin transitions. In many cases, elastic interactions between the SC units are strong enough to induce hysteresis at the thermal spin transition[21] which occurs as a first-order phase transition. Such "switchable" molecular solids are promising in terms of optical data storage.[22] A previous report by Ohkoshi *et al.*[23] showed the feasibility of spectroscopic ellipsometry (SE) to measure the refractive index of a photomagnetic Prussian blue analog (PBA). We report here on the ability of SE to provide a quantitative determination of the HS fraction, using the example of a SC compound with hysteretic thermal transition. To demonstrate the potentiality of the SE technique for SC solids, we have chosen to use an $[Fe(NH_2\text{-}trz)_3]Br_2$ sample,[24] which was the first SC system utilized to demonstrate the potentialities of these materials in the design of molecular-based memory devices and displays.[1,25] Indeed, this SC sample presents a spin transition around room temperature, accompanied by a large hysteresis loop, where both states are stable at ambient temperature. The transition can also be reproduced many times without any alteration in the phenomenon. A remarkable color change is also observed between the LS (purple) and the HS (white) states upon the spin transition of this sample. Consequently, we expect a sufficient difference between the ellipsometric signals associated with the HS and LS phases, leading to easy characterization. The paper is organized as follows. In Sec. II, we describe sample preparation, the ellipsometric setup, and the methodology of the spectroscopic ellipsometry; in Sec. III, we give the experimental results; in Sec. IV, we discuss application of the Kramers-Kronig (KK) relations. Then we end in Sec. V with a discussion and conclusions.

II. EXPERIMENTS

A. Sample preparation

Pellets of the sample $[Fe(NH_2\text{-}trz)_3]Br_2$ were prepared from the powder, and pressed under 10 kbar for one minute. The pellet diameter is of 5 mm and its thickness is ~1 mm. To ensure the homogeneity of the surface of the pellet, we pressed it using an optical polished piston. Preliminary experiments showed that both states are obtained reversibly on

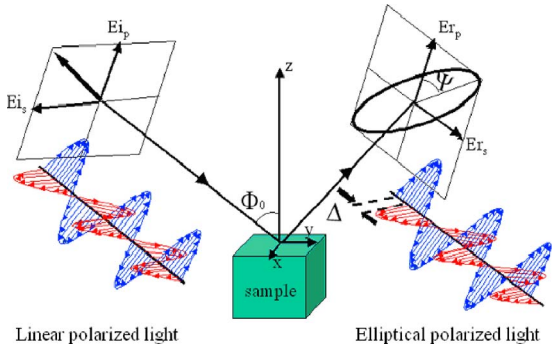

FIG. 1. (Color online) Schematic illustration of SE measurement. After reflection under an incident angle Φ_0 from the sample, the change in polarization is measured via the ellipsometric angles ψ and Δ. E_{is} (E_{rs}) and E_{ip} (E_{rp}) are, respectively, the *s*- and *p*-polarized electric field vectors of the incident (reflected) light.

changing the temperature. Therefore, the application of pressure has not altered the SC phenomenon.

B. Spectroscopic ellipsometry: Method and setup

SE is an excellent technique to investigate the optical properties of solids. It is a surface-sensitive and nondestructive technique used not only to determine optical constants of bulk materials, but also to characterize any layered structures and surface changes.[26,27] SE is based on measurement of the polarization of a beam of light reflected from the surface of the sample at a known angle of incidence (see Fig. 1 for a schematic illustration). Thus, no reference samples are needed for calibration. Two parameters (ψ,Δ) are measured as functions of wavelength and the angle of incidence, as seen in Fig. 1. These parameters are related to the ratio of the reflection coefficients of the sample, r_p and r_s, respectively, associated with *p*-polarized (parallel to the plane of incidence) and *s*-polarized light (perpendicular to the plane of incidence),[28] given by

$$\rho = \frac{r_p}{r_s} = \tan(\psi)e^{i\Delta}. \tag{1}$$

To derive the complex refractive index $\tilde{n}=n+jk$, we use a semi-infinite model,[27] which allows us to establish a relation between the ellipsometric parameters (ψ,Δ) and the indices n and k as a function of the complex reflectance ratio ρ, through

$$n + jk = n_0 \sin\Phi_0 \sqrt{1 + \left(\frac{1-\rho}{1+\rho}\right)^2 \tan^2\Phi_0}, \tag{2}$$

where n_0 (=λ) and Φ_0 are, respectively, the refractive index of the vacuum and the incidence angle.

SE measurements on a SC $[Fe(NH_2\text{-trz})_3]Br_2$ pellet sample have been performed in the 240–1000 nm optical range at an incident angle of 70° (near the Brewster angle), using a UVISEL spectroscopic phase-modulated ellipsometer. This ellipsometer incorporates photoelastic device[29,30] to modulate the polarization of light, and we have used as light source a 150 W Xe short arc lamp. Calcite prism polarizers are used to polarize the incident beam and to analyze the light beam reflected by the sample. To control the temperature of the sample, we used a temperature controller (Linkam TMS 94) which allows sample characterization in the range 77–873 K. This device is adapted for Jobin-Yvon ellipsometry by a THMS600 heating-cooling stage. The stage contains a large-area temperature-controlled element with a platinum resistor sensor embedded close to the surface for accurate temperature measurements. We could program this temperature controller in ramps from 260 to 360 K with a temperature step of 5 K, and time pauses of 3 min in order to accumulate the optical spectrum. The sample is placed in a chamber under a controlled atmosphere of nitrogen. It is simply mounted in direct contact with a highly polished silver heating element to ensure an efficient heat transfer and homogeneity. A platinum resistor sensor allows a temperature measurement with an accuracy of 0.1 K. The light spot on the sample has a size of ~1–2 mm diameter, and it probes always the same region of the sample. Different experiments realized at constant temperature, probing different regions of the sample, have given the same result. This excludes the existence of large inhomogeneities of temperature in the sample.

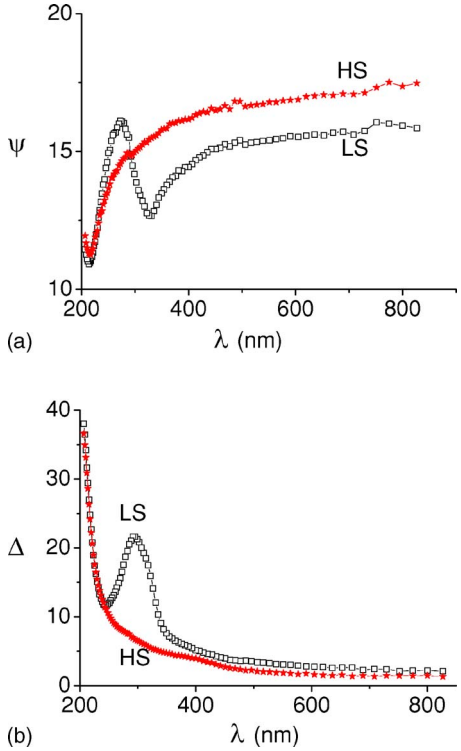

FIG. 2. (Color online) Wavelength dependences of the ellipsometric parameters ψ (a) and Δ (b) in the HS state at 353 K (⋆), and in the LS state at 263 K (□), near the pseudo-Brewster angle (70°).

III. RESULTS AND DISCUSSION

A. Thermal characterization of HS and LS states

The wavelength dependences of ψ and Δ in the HS and LS regions are displayed in Fig. 2. The HS and LS states

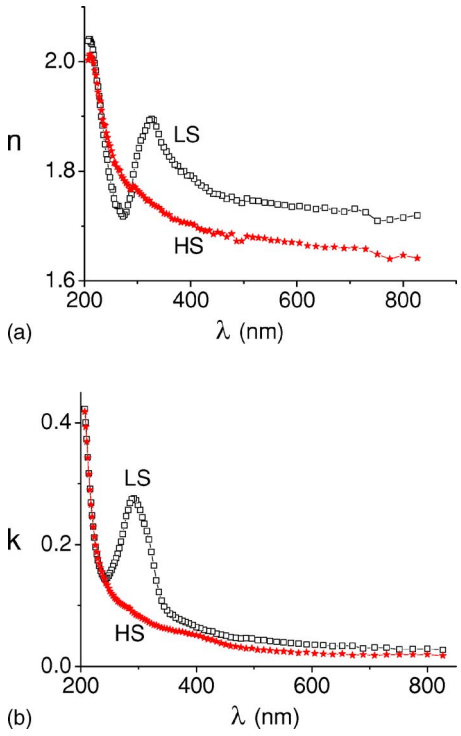

FIG. 3. (Color online) Extracted wavelength dependences of n (a) and k (b) using data of Fig. 2 and Eq. (2) in the HS state, at 353 K (⋆), and in the LS state at 263 K (□), near the pseudo-Brewster angle (70°).

were respectively characterized at 353 and 263 K. The obtained spectra clearly show that the ellipsometric responses in the LS and HS states are very different, indicating that SE well characterizes the two spin states. Indeed, ψ versus wavelength in the LS state shows the existence of an electronic resonance, located around 300 nm, while it disappears in the associated spectra of the HS state. Starting from the experimental results of Fig. 2 and using Eq. (2), we derive the wavelength dependence of the indices n and k in the HS and LS states. The results are shown in Fig. 3. It is worth mentioning that at 263 K, i.e., in the LS state, one absorption band is observed in the extinction coefficient k, at 298 nm. We assign this band to metal-ligand charge-transfer transitions[40] (MLCTs) from the $^1A_1$ level to the T_1 level in the LS state. This transition is not found in the HS state (at 353 K). It is well known that the absorption coefficient k is weakly affected by the scattering processes. However, the refractive index n is more sensitive to the change in the roughness of the surface caused by the SC transition. Therefore, we expect a dependence of the associated spectra on the mechanical stress at the surface. The latter can be temperature dependent, due to the volume change upon the spin-crossover transition, as observed in Fig. 3(a), where the baseline of the spectra shifts with temperature.

In order to check the accuracy of the SE ellipsometry data, we have also investigated the absorbance properties on the same system using uv-visible absorption measurements. We performed the experiment on KBr pellets using a Varian CARY 5E double-beam spectrophotometer, equipped with a Eurolabo cryostat (Model No. 21525) and a Specac temperature controller (Model No. 20120). The measured spectra at 265 and 315 K, corresponding, respectively, to the LS and HS states, are presented in Fig. 4. To compare SE predictions with those of the present absorption data, we first determined the absorption coefficient α from the extinction coefficient $k(\lambda)$ [see Fig. 3(b)] using the textbook relation $\alpha(\lambda) = 4\pi k(\lambda)/\lambda$. We found that SE allows us to reproduce the main qualitative features of the optical spectra. In particular, the transition band at 300 nm is in very good agreement with that observed by SE, depicted in Fig. 3(b). In addition, the isobestic point located at 240 nm is well reproduced by both methods. The quantitative comparison between the two experimental methods is not made in the present work, for the following reasons: (i) spectrophotometer experiments are done in transmission and not in reflection as in the SE measurements; (ii) the sample used for spectrophotometry investigations is diluted with KBr and then pressed in order to have a transparent pellet. Despite these differences between the two experimental procedures, the results are qualitatively similar. Therefore, we will use the extinction coefficient $k(\lambda)$ as a reference point, weakly dependent on scattering processes, in order to correct the experimental refractive index n.

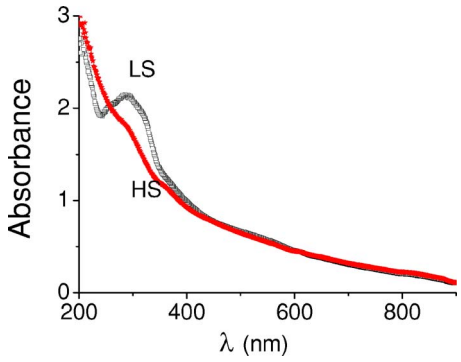

FIG. 4. (Color online) Spectrophotometer absorption spectra of [Fe(NH_2-trz)$_3$]Br_2 diluted in KBr, in the LS (263 K, □) and HS (353 K, ⋆) states. The obtained transition band at $\lambda = 300$ nm in the LS state, is in very good agreement with SE results [see Fig. 3(b)].

B. Thermal evolution of the HS fraction

Now, we investigate the thermal properties of our SC pellet sample by means of SE at different temperatures. To derive the HS fraction, that is, the fraction of molecules in the HS state, we use the extinction coefficient $k(\lambda)$ which is less affected by scattering than the refractive index $n(\lambda)$, as we previously explained. The thermal evolutions of the refractive index spectrum $n(\lambda)$ and that of the extinction coefficient $k(\lambda)$ at different temperatures between 263 and 358 K are shown in Fig. 5, in the warming process. There, we have evidenced that the spectra follow a regular and monotonic behavior with temperature, with the existence of two isobestic points around ~230 and ~290 nm. Moreover, on the associated spectra of $n(\lambda)$, the baseline moves from $n = 1.70$ (LS) to $n = 1.65$ (HS). We interpret this shift as an indication of the existence of scattering effects. In contrast,

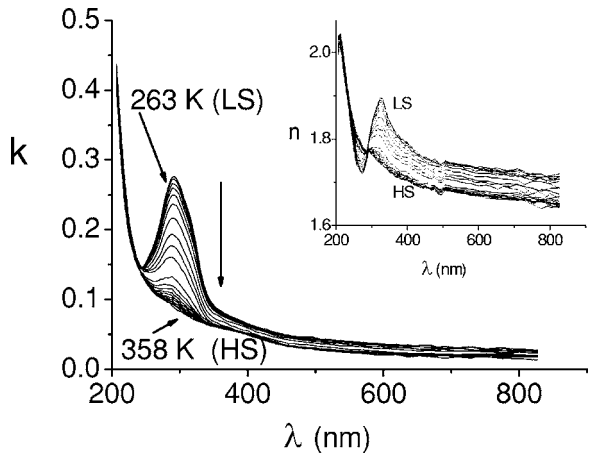

FIG. 5. Thermal evolution of the absorption spectra $k(\lambda)$ of a pellet sample of $[Fe(NH_2\text{-}trz)_3]Br_2$ in the heating process from 263 (LS) up to 358 K (HS). An isobestic point at $\lambda=240$ nm and a MLCT band at $\lambda=300$ nm are evidenced. In the inset is depicted the thermal evolution of $n(\lambda)$.

and in agreement with our previous predictions, this effect remains quite small in the thermal evolution of the absorption spectra $k(\lambda)$. Remarkably, the absorption spectra also show an isobestic point at $\lambda=240$ nm, which remains invariant in the cooling and warming processes.

Thus, the HS fraction, denoted by n_{HS}, can be determined using different approaches: (i) in the first approach, n_{HS} is assumed as proportional to the area of the absorption spectra $k(\lambda)$ relative to the HS state (see Fig. 6); (ii) in the second attempt n_{HS} can be assumed as proportional to the intensity of the absorption peak located at $\lambda=300$ nm at different temperatures; and finally (iii) the HS fraction can also be extracted from the examination of the refractive index $n(\lambda)$, by using the same protocol.

In this work, we consider the first approach. Let us denote by $A(T)$ the area situated between the absorption spectra at temperature T and the absorption line of the HS state (see Fig. 6). The HS fraction n_{HS} is then calculated as

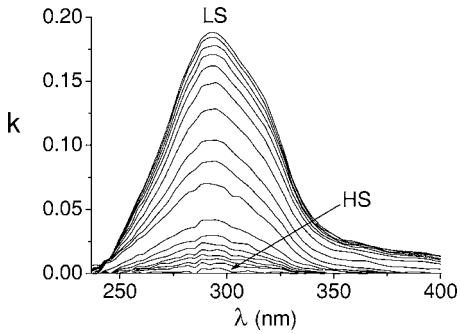

FIG. 6. Thermal evolution of the SE absorption band (240–400 nm) of $[Fe(NH_2\text{-}trz)_3]Br_2$ in the heating process from 263 (LS) to 358 K (HS). The temperature change between two neighboring curves is 5 K. Note that all the curves merge at the isobestic point located at $\lambda=240$ nm.

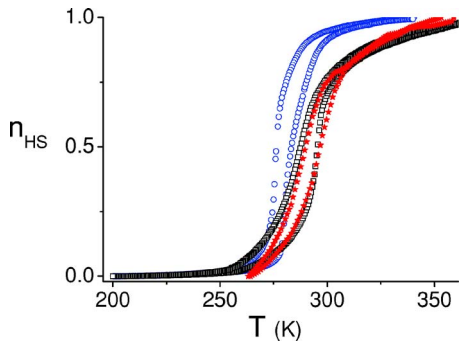

FIG. 7. (Color online) Thermal hysteresis loops of $[Fe(NH_2\text{-}trz)_3]Br_2$ sample. The magnetic measurements are depicted by ○ for the powder sample and by □ for the pellet. SE measurements on the same pellet are shown by ⋆.

$$n_{HS}(T) = 1 - \frac{A(T)}{A_{LS}}, \tag{3}$$

where A_{LS} is the surface associated with the LS state, obtained at $T=263$ K. In practice, the analysis is made in the range of wavelengths going from 240 to 400 nm.

The thermal evolution of the HS fraction, illustrated in Fig. 7, obtained after integrating the previous spectra of Fig. 6, clearly shows the existence of a thermal hysteresis loop centered around 293 K, with an associated width of 8 K.

To check the accuracy of the SE technique, we compare quantitatively the present results with those obtained by magnetic measurements. As for the magnetic experiments, we have characterized both powder and pellet samples. The thermal dependences of the obtained HS fractions are depicted in Fig. 7. A hysteresis loop, with an associated width of $\simeq 8$ K, is obtained in both cases. A very good agreement is found between SE and magnetic data on the same pellet sample. However, both hysteresis loops are shifted to higher temperature, when compared with that of the powder sample. This behavior denotes the existence of a residual pressure inside the pellet sample. Based on a simple theoretical approach,[31] it is easy to demonstrate that the effect of pressure p on the transition temperature is given by $T_{1/2}(p)=T_{1/2}(0)+p|\Delta V|/\Delta S$, where $T_{1/2}(0)$ is the transition temperature of the powder sample, ΔV is the volume change, and ΔS is the entropy change at the transition. The ratio $|\Delta V|/\Delta S$ can be obtained from the study of the phase diagram (T,p) of the system,[32] using reflectivity measurements. Typical values of 20 K/kbar are obtained for the previous ratio in the case of SC and PBA.[34] Evaluating the shift in the transition temperature as equal to 8 K, we find a residual pressure of 0.4 kbar in the pellet sample, which is small in comparison with the applied pressure of 10 kbar, used to prepare the pellet sample. It is worth noting that the pressure effect on SC solids is not always trivial. Indeed, in many SC systems, it was observed that applied pressure may induce a nonmonotonic shift[35] in the transition temperature. In addition, it also acts on the shape of the thermal transition curve.

For example, on the sample $[Fe(btr)_2(NCS)_2]\cdot H_2O$, experimental data resulting from reflectivity measurements un-

der pressure[33,34] yields to an upward monotonic shift of the hysteresis loop. In contrast, recent x-ray studies[36] evidencing for the first time the formation of spinlike domains upon the spin-crossover transition have shown, in accordance with magnetic measurements performed by the authors, that the same compound embodied in vacuum grease leads to a downward shift of the whole hysteresis loop by 2 K, in comparison with the grease-free sample. The nonlinear effect of pressure has also been reported in quasi-one-dimensional SC solids,[37,38] in which the transition temperature first increases for low applied pressures and then starts to decrease from some threshold value of applied pressure.

Let us now discuss in more detail the magnetic and SE data of Fig. 7 corresponding to the pellet sample. Remarkably, SE ellipsometry was able to find two important aspects of this SC sample: (i) the first aspect concerns the thermally bistable character of this SC solid, for which SE well reproduces the shape and the width of the associated hysteresis loop; (ii) the second aspect is the location of the transition temperature, which is also well reproduced.

Here, it is also important to mention that the magnetic and SE measurements were performed using different temperature kinetics. In the SE experiments we changed the temperature using a rate of 0.7 K/min, while in the superconducting quantum interference device SQUID we used 0.3 K/min. Therefore, we expect a larger hysteresis from the SE data due to the kinetic effect. However, the small discrepancy observed in Fig. 7 shows that magnetic hysteresis is wide and less regular than that obtained by SE. Moreover, it is admitted that SE provides information from the surface of the sample, while magnetic measurement is a volume response. However, remarkably, the two hysteresis loops match each other quite well. Thus, it becomes interesting to discuss the reason of this unexpected good agreement. It is worth noticing that SE collects information on sample layers situated in some penetration depth $\delta(\lambda)$, given in a first approximation by $\delta(\lambda) \simeq 1/\alpha(\lambda) = \lambda/4\pi k(\lambda)$, where $\alpha(\lambda)$ is the absorption coefficient of the sample. In the region corresponding to the maximum of the ellipsometric signal, that is, the region $\lambda \in [250\ \text{nm}:350\ \text{nm}]$, we evaluate $\delta \approx 50$ nm. Knowing that the distance between two atomic layers in SC solids, that is, the distance between two consecutive iron atoms, is ~ 1 nm, it follows that for the present sample the SE probes more than 50 atomic layers for the wavelength used of $\lambda = 300$ nm, which corresponds to a mesoscopic scale. Therefore, we can consider this result as a plausible reason for the good agreement between SE and magnetic data. Moreover, recent results[39] have shown that SC nanoparticles of 50–60 nm size give the same magnetic response as macroscopic samples, which is in good agreement with our SE results. Finally, the hysteresis loop obtained by SE is not due to kinetic effects, but it really reflects the interactions between the SC units.

IV. APPLICATION OF KRAMERS-KRONIG RELATIONS

To prove that scattering phenomena are present in the uv-visible region, due to surface roughness, we use the well-known KK equations, which establish a connection between the real and imaginary parts of the complex index $\tilde{n}$. These relations are also known as dispersion relations, which were first introduced by Kronig,[41] and are a direct consequence of the causality principle. In the present case, the real and imaginary parts of the complex index satisfy the KK relations,[42,43] given by

$$n(\omega) = 1 + \frac{2}{\pi} \mathrm{P} \int_0^\infty \frac{\omega' k(\omega')}{\omega'^2 - \omega^2} d\omega', \tag{4}$$

and

$$k(\omega) = -\frac{2\omega}{\pi} \mathrm{P} \int_0^\infty \frac{n(\omega') - 1}{\omega'^2 - \omega^2} d\omega', \tag{5}$$

where P is the Cauchy principal value of the integral, and ω is the frequency. Combining the KK relations [Eqs. (4) and (5)] with the experimental spectra of the absorption coefficient $k(\lambda)$ in the LS and HS sates as input data, we calculate the refractive index n_{calc}, in both states and compare it with the experimental data, given in Fig. 3(a). The results are summarized in Figs. 8(a) and 8(c), where we distinguish two regions in both states (LS, HS). In the visible region, the calculated refractive index $n_{\text{calc}}(\lambda)$, reproduces very well the experimental data $n_{\text{expt}}(\lambda)$. In contrast, an important discrepancy is observed in the uv region, where it is enhanced at short wavelengths, for which we expect that surface effects are predominant in the SE signal of $n(\lambda)$.

A quantitative analysis of the λ dependence of the difference $(n_{\text{expt}} - n_{\text{calc}})$ between the experimental and the calculated refractive indices (using the KK relations), gives rise to the following empirical relation between n_{expt}, n_{calc}, and the wavelength λ, which is valid at all temperatures,

$$n_{\text{expt}}(\lambda) = n_{\text{calc}}(\lambda) + \frac{a}{\lambda - b}. \tag{6}$$

It is worth noting that the parameters a and b involved in Eq. (6) have the dimension of the wavelength λ. Here, the quantity b represents the cutoff in wavelength of the optical spectra, for which the calculated refractive index diverges due to the presence of a huge absorption around $\lambda = 190$ nm. Therefore, we expect this value to be temperature independent. The parameter a accounts for the discrepancy between $n_{\text{expt}}(\lambda)$ and $n_{\text{calc}}(\lambda)$. Actually, when $a = 0$ we have $n_{\text{expt}}(\lambda) = n_{\text{calc}}(\lambda)$. Thus, we consider the parameter a as related to the mean value of the roughness at the surface, which we denote by R_q. To derive this important quantity, we investigated the surface topography of the pellet sample using atomic force microscopy (AFM) measurements and we found $R_q = 19$ nm in a scan area of $5 \times 5\ \mu\text{m}^2$ at ambient temperature in the LS state. It is important to mention that the ratio $R_q/\lambda \approx 0.1$ remains quite small, even in the uv region.

The best agreement between the calculated and the experimental curves is then obtained for $b = 192$ nm. Indeed, as shown in Figs. 8(b) and 8(d), the same empirical law was able to show the scattering effect in the LS and HS states.

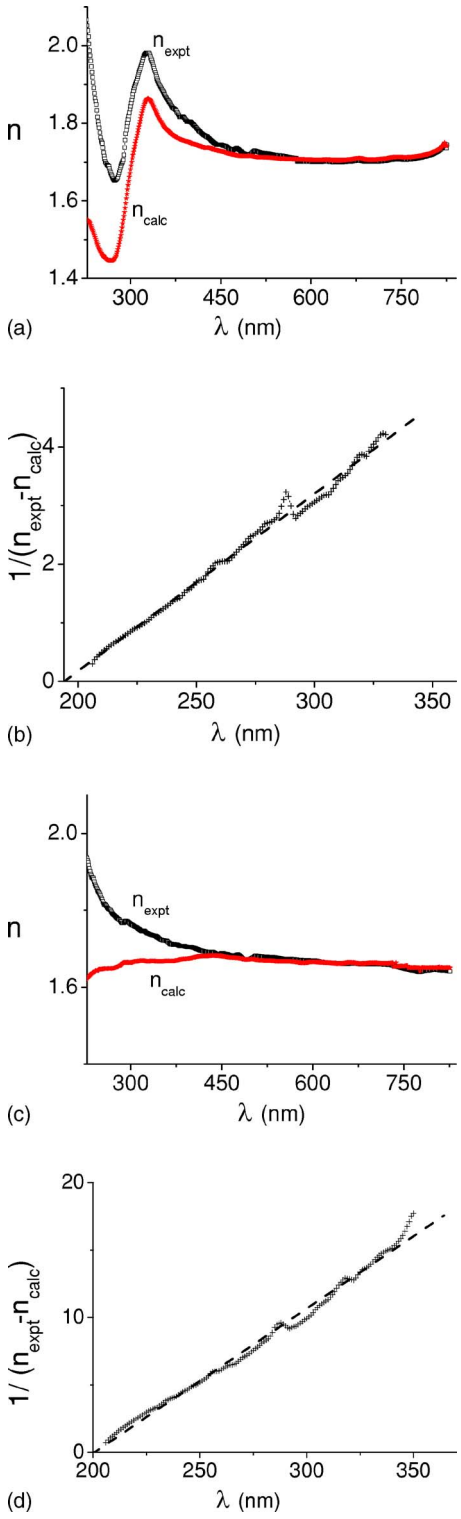

FIG. 8. (Color online) Wavelength dependence of the experimental (n_{expt}, □) and the calculated (n_{calc}, ⋆) refractive index in the LS (a) and HS (c) states. In both states LS (b) and HS (d), the wavelength dependence of the inverse of ($n_{expt}-n_{calc}$) (+) follows a linear behavior. The dashed line is the best fitting.

Table I, summarizing the results obtained at different temperatures, shows that the parameter $a \propto R_q$ depends on the spin state (HS, LS) and therefore on the volume change upon the spin-crossover transition. Actually, we found $a=11.5$ (10) nm in the LS (HS) state, in quite good agreement with the volume expansion of the SC molecules, which affects the morphology of the surface, by changing its roughness. However a more rigorous quantitative analysis of roughness effects needs temperature-dependent AFM investigations on thin films of SC materials, which is beyond the scope of the present paper.

TABLE I. Numerical values of the parameters a and b at different temperatures. Both parameters are extracted from the analysis of the experimental curves of the refractive index n, following Eq. (6).

	Temperature (K)					
Parameter	263 (LS)	278	293	308	353	358 (HS)
a (nm)	11.5	11.5	11	11	10	10
b (nm)	191.5	192	192	192	192	192

V. CONCLUSION

Spectroscopic ellipsometry at different temperatures was used to investigate the thermal properties of a pellet sample of the spin-crossover compound $[Fe(NH_2\text{-}trz)_3]Br_2$. This sample was first analyzed by magnetic measurements in its powder and pellet forms, and we found the existence of a residual pressure of 0.4 kbar in the pellet form, which shifts the hysteresis loop by 8 K at higher temperature. From the wavelength dependence of the SE angles ψ and Δ, and using a semi-infinite model, we extracted the wavelength dependence of the refractive index n and that of the extinction coefficient k at different temperatures. There, we found that the LS state presents a strong absorption at 300 nm, related to the existence of a MLCT band in the uv region of $k(\lambda)$. We used this band as a LS marker, and we evaluated quantitatively the HS fraction by integrating the absorption spectra. We then derived the thermal behavior of the HS fraction, which we found in excellent agreement with the magnetic data on the same sample. We also investigated the global consistency of the optical data by application of the KK relations, which are well obeyed above 450 nm. In contrast, at lower wavelengths we observed large discrepancies, which are discussed in terms of sample roughness. We found that they can be modeled using a simple empirical formula, involving the lower cutoff in wavelength of the optical spectra and the average surface roughness. Finally, this work clearly shows that SE is a useful technique for characterizing and evaluating the HS fraction in SC solids. These results show that SE is also sensitive to mechanical stress and constitutes a very promising technique of investigations of thermo- and photoswitchable solids under external constraints, such as pressure, light, magnetic field, etc. In particular, we expect that this technique will be relevant to investigate the physical properties of thin films and nanoparticles dispersed in gel, for example, of thermo- and photochromic switchable materials, such as SC solids, Prussian blue analogs, or even organic charge transfer crystals.[44]

ACKNOWLEDGMENTS

This work was supported by the Ministère de l'Education Nationale (PPF contract), CNRS, Université de Versailles Saint-Quentin-en-Yvelines, and Conseil Régional d'Ile de France, which we deeply acknowledge. We also warmly acknowledge Frederic Mourgues for technical help, J. Laverdant, T. Hamon, and M.L. Boillot for useful discussions.

*Electronic address: kbo@physique.uvsq.fr

[1] P. Gütlich, Struct. Bonding (Berlin) **44**, 83 (1981).
[2] O. Kahn and J. P. Launay, Chemtronics **3**, 140 (1988).
[3] J. Jeftic and A. Hauser, J. Phys. Chem. B **101**, 10262 (1997).
[4] G. Molnár, V. Niel, J.-A. Real, L. Dubrovinsky, A. Bousseksou, and J. McGarvey, J. Phys. Chem. B **107**, 3149 (2003).
[5] S. Decurtins, P. Gütlich, C. P. Köhler, H. Spiering, and A. Hauser, Chem. Phys. Lett. **105**, 1 (1984).
[6] P. Gütlich, A. Hauser, and H. Spiering, Angew. Chem., Int. Ed. Engl. **33**, 2024 (1994).
[7] S. Bonhommeau, G. Molnár, A. Galet, A. Zwick, J.-A. Real, J. J. McGarvey, and A. Bousseksou, Angew. Chem., Int. Ed. **44**, 4069 (2005).
[8] N. O. Moussa, G. Molnár, S. Bonhommeau, A. Zwick, S. Mouri, K. Tanaka, J. A. Real, and A. Bousseksou, Phys. Rev. Lett. **94**, 107205 (2005).
[9] S. Decurtins, P. Gütlich, K. M. Hasselbach, A. Hauser, and H. Spiering, Inorg. Chem. **24**, 2174 (1985).
[10] A. Bousseksou, K. Boukheddaden, M. Goiran, C. Consejo, M-L. Boillot, and J-P. Tuchagues, Phys. Rev. B **65**, 172412 (2002).
[11] E. König, Struct. Bonding (Berlin) **76**, 51 (1991).
[12] O. Kahn, Curr. Opin. Solid State Mater. Sci. **1**, 547 (1996).
[13] J. Krober, E. Codjovi, O. Kahn, F. Grolière, and C. Jay, J. Am. Chem. Soc. **115**, 9810 (1993).
[14] B. Gallois, J.-A. Real, C. Hauw, and J. Zarembowitch, Inorg. Chem. **29**, 1152 (1990).
[15] E. W. Müller, J. Ensling, H. Spiering, and P. Gütlich, Inorg. Chem. **22**, 2074 (1983).
[16] G. Vos, R. A. Le Fèbre, R. A. G. de Graff, J. G. Haasnoot, and J. Reedijk, J. Am. Chem. Soc. **105**, 1682 (1983).
[17] E. König, G. Ritter, S. K. Kulshreshtha, J. Waigel, and H. A. Goodwin, Inorg. Chem. **23**, 1896 (1984).
[18] E. König, G. Ritter, H. Grünsteudel, J. Dengler, and J. Nelson, Inorg. Chem. **33**, 837 (1994).
[19] V. Ksenofontov, H. Spiering, A. Schreiner, G. Levchenko, H. A. Goodwin, and P. Gütlich, J. Phys. Chem. Solids **60**, 393 (1999).
[20] A. Bousseksou, G. Molnár, P. Demont, and J. Mengotto, J. Mater. Chem. **13**, 2069 (2003).
[21] O. Kahn, *Molecular Magnetism* (VCH, New York, 1993).
[22] O. Kahn, J. Krober, and C. Jay, Adv. Mater. (Weinheim, Ger.) **11**, 4 (1992).
[23] S. Ohkoshi, T. Nuida, T. Matsuda, H. Tokoro, and K. Hashimoto, J. Mater. Chem. **15**, 3291 (2005).
[24] O. Kahn and E. Codjovi, Philos. Trans. R. Soc. London, Ser. A **354**, 359 (1996).
[25] J. Zarembowitch and O. Kahn, New J. Chem. **15**, 181 (1991).
[26] R. M. A. Azzam and N. M. Bashara, *Ellipsometry and Polarized Light* (North-Holland, Amsterdam, 1977).
[27] H. G. Tompkins and W. A. McGahan, *Spectroscopic Ellipsometry and Reflectometry* (John Wiley & Sons, New York, 1999).
[28] B. Drevillon, J. Perrin, R. Marbot, A. Violet, and J. L. Dalby, Rev. Sci. Instrum. **53**, 969 (1982).
[29] S. N. Jasperson and S. E. Schnatterly, Rev. Sci. Instrum. **40**, 761 (1969); S. N. Jasperson, D. K. Burge, and R. C. O'Handley, Surf. Sci. **37**, 584 (1973).
[30] G. R. Boyer, B. F. Lamouroux, and B. S. Prade, Appl. Opt. **18**, 1217 (1979).
[31] E. Codjovi, J. Jeftic, N. Menendez, and F. Varret, C.R. Acad. Sci., Ser. IIc: Chim **4**, 181 (2001).
[32] J. Jeftic, N. Menendez, A. Wack, E. Codjovi, J. Linares, A. Goujon, G. Hamel, S. Klotz, G. Syfosse, and F. Varret, Meas. Sci. Technol. **10**, 1059 (1999).
[33] E. Codjovi, N. Menendez, J. Jeftic, and F. Varret, C.R. Acad. Sci., Ser. IIc: Chim **4**, 181 (2004).
[34] A. Sava, C. Enachescu, A. Stancu, K. Boukheddaden, E. Codjovi, I. Maurin, and F. Varret, J. Optoelectron. Adv. Mater. **5**, 977 (2003).
[35] H. Spiering, K. Boukheddaden, J. Linares, and F. Varret, Phys. Rev. B **70**, 184106 (2004).
[36] S. Pillet, J. Hubsh, and C. Lecomte, Eur. Phys. J. B **38**, 541 (2004). See also S. Pillet, V. Legrand, M. Souhassou, and C. Lecomte, Phys. Rev. B **74**, 140101(R) (2006).
[37] E. König, G. Ritter, J. Waigel, and H. Goodwin, J. Chem. Phys. **83**, 3055 (1986).
[38] K. Boukheddaden, S. Miyashita, and M. Nishino, Phys. Rev. B **75**, 094112 (2007).
[39] J. F. Létard, P. Guionneau, and L. Goux-Capes, Top. Curr. Chem. **235**, 221 (2004).
[40] S. Decurtins, P. Gütlich, K. M. Hasselbach, A. Hauser, and H. Spiering, Inorg. Chem. **24**, 2174 (1985).
[41] R. Kronig, J. Opt. Soc. Am. **12**, 547 (1926).
[42] H. A. Kramers, Nature (London) **117**, 775 (1926).
[43] R. Kronig, Ned. Tijdschr. Natuurkd. **9**, 402 (1942).
[44] E. Collet, M. H. Lemée Cailleau, M. Buron-Le Cointe, H. Cailleau, M. Wulff, T. Luty, S. Koshihara, M. Meyer, L. Toupet, P. Rabiller, and S. Techert, Science **300**, 612 (2003).